Organic Process Research & Development **2004**, *8*, 488–494

Monitoring and Feedback Control of Supersaturation Using ATR-FTIR to Produce an Active Pharmaceutical Ingredient of a Desired Crystal Size

Vincenzo Liotta* and Vijay Sabesan

Schering-Plough Research Institute, 1011 Morris Avenue, Union, New Jersey 07083, U.S.A.

Abstract:

Automation, in situ monitoring, and process control tools are implemented to understand and control the crystallization of an active pharmaceutical ingredient in development. As a first step in the study, the metastable zone is generated automatically by linking a laser backscattering probe to an automated laboratory reactor. Using the metastable zone as a guide, crystallization experiments with varying cooling rates and seeding protocols are conducted and monitored. The evolution of solution concentration and supersaturation is determined by transmitting data from an in situ total reflectance Fourier transform infrared (ATR-FTIR) spectroscope to the laboratory reactor. Supersaturation profiles coupled with data from the laser backscattering probe demonstrate the prevalence of primary and secondary crystal nucleation in the process. A cascaded proportional-integral controller is tuned and implemented to promote crystal growth over nucleation by maintaining supersaturation at low constant values. Nonlinear temperature profiles that result in crystals of larger size are thereby generated.

1. Introduction

Crystallization is widely used in pharmaceutical processes as a purification operation that results in a solid product. In the production of the active pharmaceutical ingredient (API), product properties such as the crystal size distribution, polymorphism, and morphology are defined in the crystallization step. These properties, in turn, may have a large impact on the downstream unit operations such as filtration and drying, as well as the biopharmaceutical characteristics of the drug product.

Given the importance of crystallization, it is clear that understanding and controlling the underlying mechanisms (nucleation and growth) and the principal driving force of the process (supersaturation) are essential. Recently, the realization of these objectives has been facilitated by several factors. On the technological side, advances in the robustness and accuracy of in situ sensors combined with automation make it possible to implement real-time process monitoring and control. The incentive to implement these strategies in the pharmaceutical manufacturing arena has also increased following the FDA's initiative on Process Analytical Technology.

Although the implementation of real-time feedback control of pharmaceutical crystallization in a manufacturing process is not yet commonplace, recent laboratory examples of supersaturation monitoring and control in the literature demonstrate the possibilities.[1−3]

This contribution discusses the cooling crystallization of pharmaceutical compound N, a Schering-Plough API drug candidate in the early development stages. During laboratory process development studies, the crystallization process was observed to generate material of a wide range of crystal sizes. The study described in this report was initiated with the objective of understanding and controlling the crystallization of compound N to produce material within a desired crystal size range by applying automation tools, in situ measurement technologies, and feedback control algorithms.

2. Experimental Methods

2.1. Experimental Procedure. The crystallization procedure used in this work involved the dissolution of the starting material in 10 volumes of toluene (i.e. 10 mL of toluene per gram of starting material) at 70 °C, followed by cooling to 20 °C. Seeding was performed in some of the experiments. The resulting product crystals were filtered and dried in a vacuum tray oven at 20 °C to yield final product.

2.2. Equipment, Sensors, and Communication. Experiments were carried out in a 1-L glass HEL (Hazard Evaluation Laboratory) AutoLab running under WinISO 2.2.25 software. A custom-designed glass lid supported the agitator shaft, thermocouple, feed, and in situ probes. All experiments were agitated at 200 rpm with a retreating curve impeller. Temperature control was achieved by a Huber Unistat 360-W heater/chiller circulating through the AutoLab jacket.

Solution concentration in the reactor was determined via attenuated total reflectance Fourier transform infrared (ATR-FTIR) spectroscopy. A Mettler-Toledo ReactIR 1000 running v2.21 software with a DiComp immersion probe was used. The probe was introduced into the reactor at an approximately 18° angle (from vertical) to the agitation flow to minimize fouling at the probe tip. IR spectra were collected at intervals of 23 s with each spectrum averaged over 10 scans. A ReactIR software macro produced a digital signal proportional to a user-selected ReactIR variable (concentration, in this case). This signal was transformed into an analogue output via a D/A converter and transmitted to the AutoLab, where it was scaled and converted back to the

* To whom correspondence should be addressed. E-mail: vincenzo.liotta@spcorp.com.

(1) Feng, L.; Berglund, K. A. *Cryst. Growth Des.* **2002**, *2*, 449.
(2) Fujiwara, M.; Chow, P. S.; Ma, L. M.; Braatz, R. D. *Cryst. Growth Des.* **2002**, *2*, 363.
(3) Gron, H.; Borissova, A.; Roberts, K. J. *Ind. Eng. Chem. Res*. **2003**, *42*, 198.

Published on Web 05/06/2004
10.1021/op049959n CCC: $27.50

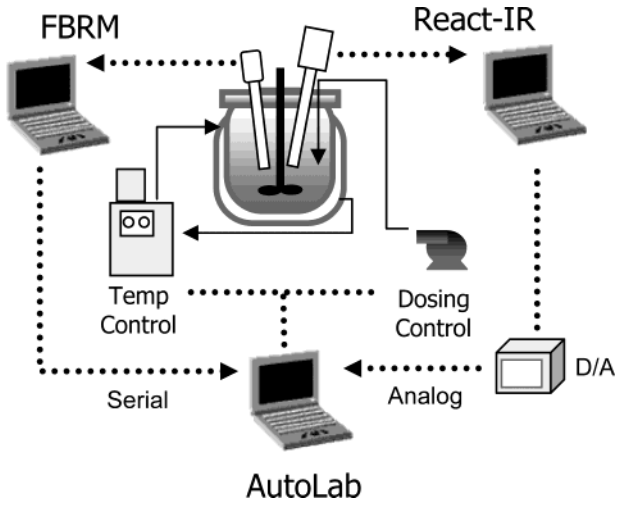

Figure 1. **Schematic of the equipment and sensors used in this work.**

original value. The concentration data and the reactor temperature were used to calculate supersaturation via a calculation block in the AutoLab software.

A Lasentec FBRM D600L was used to monitor particle chord length and counts using 6.0 build 13a software. As with the ReactIR, the probe was introduced into the reactor at an angle to minimize probe fouling. Communication between the FBRM computer and the AutoLab computer was enabled via an RS232 interface. In this way, up to eight different particle statistics were sent from the FBRM to the AutoLab digitally.

A schematic showing the interaction between the AutoLab (the control center), its associated equipment, and the two in situ probes is shown in Figure 1.

3. Automated Metastable Zone Determination

Identifying the metastable zone is usually the first step in crystallization development as it provides the operating envelope to favor crystal growth over nucleation or vice versa. In cooling crystallizations for example, maintaining the solution concentration profile within the metastable zone and close to the solubility curve promotes crystal growth.

Determining the metastable zone for cooling crystallizations requires some attention, as the metastable zone width is typically a function of the cooling rate employed,[2,4] and can be a function of the thermal history of the solution.[5] In all cases, the most accurate data are obtained by using slow heating and cooling rates on a system with good temperature control. Unless automation is applied, precise determination of the metastable zone can be a tedious process.

Previous research has demonstrated the use of a laser backscattering probe (Lasentec FBRM) to determine the metastable zone.[6] Automating the technique (referred to as "AutoMeta") simply requires a link that enables the crystallizer to respond to FBRM data in real-time, as discussed below.

(4) Parsons, A. R.; Black, S. N.; Colling, R. *Chem. Eng. Res. Des.* **2003**, *81*, 700.
(5) Hussain, K.; Thorsen, G.; Mathe-Sorenssen, D. *Chem. Eng. Sci.* **2001**, *56*, 2295.
(6) Barrett, P.; Glennon, B. *Chem. Eng. Res. Des.* **2002**, *80*, 799.

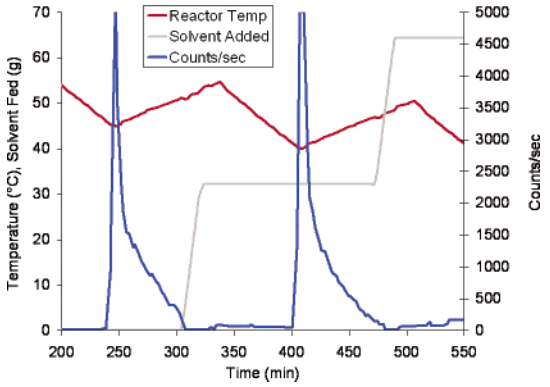

Figure 2. **Profiles of reactor temperature, solvent fed, and total counts/s for two cycles of the AutoMeta experiment.**

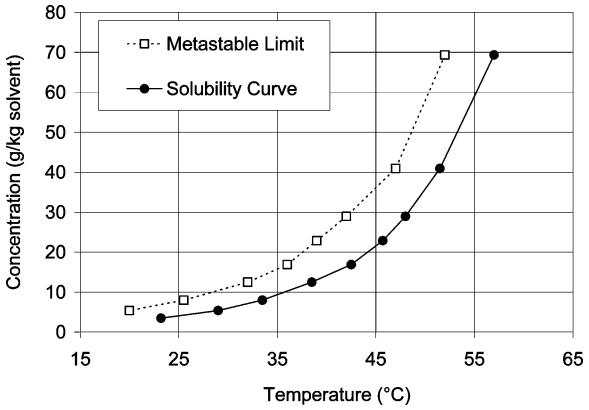

Figure 3. **Metastable and solubility curves for pharmaceutical N using the AutoMeta technique.**

The AutoMeta technique starts with a solution at a relatively high concentration held at a temperature above the solubility point. The solution is cooled slowly until crystals nucleate spontaneously at the metastable limit. The FBRM detects this event via a total particle counts/s measurement (nonweighted). When the total counts/s exceeds a preprogrammed threshold (a termination condition for the cooling step), the AutoLab program initiates a slow heating step until the total counts/s decreases to the baseline, which is the solubility point. Following this, the solution is heated to several degrees above the solubility point, and a known amount of fresh solvent is added automatically to reduce the concentration. Heating and addition of the fresh solvent ensures that (1) submicrometer nuclei dissolve and (2) unintentional seeding from solids above the liquid surface is avoided. The entire cycle is repeated automatically to generate the solubility and metastable points at lower concentrations. Although a cooling crystallization is considered here, the AutoMeta technique can be applied to antisolvent crystallizations as well.

Figure 2 shows two cycles of the AutoMeta technique applied to pharmaceutical N with heating and cooling rates of 0.2 °C/min and −0.2 °C/min, respectively. IR data from separate experiments confirmed that these heating and cooling rates were slow enough to accurately describe the metastable zone for this compound. The resulting metastable and solubility curves are shown in Figure 3. Features of the metastable zone include a relatively narrow width for a pharmaceutical compound[4] and a steep solubility curve

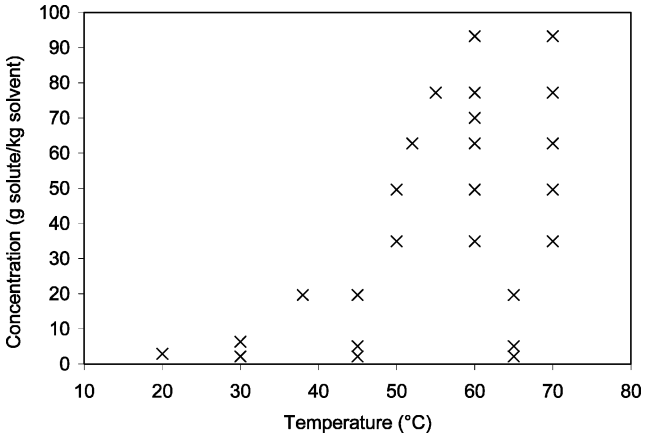

Figure 4. **Standards at different concentrations and temperatures used to develop the IR calibration.**

spanning a large range in solution concentration. These characteristics provide challenges for the monitoring and control of supersaturation, as discussed later in this work.

4. In Situ Solution Concentration

Monitoring the concentration of a solute in solution as a crystallization progresses is useful in obtaining a mechanistic understanding of the process, especially when the information is presented relative to the metastable zone. A common method to measure in situ concentration is to collect ATR-FTIR spectra at regular intervals during the crystallization.[7−10] The IR absorbance of the dissolved compound is dependent on its concentration in the solvent, as well as the temperature of the solvent.[11,12] Therefore, a calibration is necessary to convert absorbance data into solution concentration. The method of partial least squares (PLS) has been commonly used to perform such calibrations, where changes in concentration are reflected across a range of wavelengths.[13] Although the use of PLS does not produce a physical understanding of the system, it is well suited for the primary goal of prediction and estimation. For spectrometric calibrations, PLS factors are computed as linear combinations of spectral absorbances.

In this work, a PLS regression technique module developed by Mettler-Toledo (Quant-IR) was used to develop a calibration. IR absorbance spectra of solutions at several concentration levels were collected at different temperatures. A total of 26 calibration spectra (shown in Figure 4) were used as standards for the calibration model. As the IR signal was observed to be sensitive to agitator vibration, a moderate agitation speed of 200 rpm was used for all calibration points and subsequent experiments. Also, the spectral region used to develop the calibration was selected to minimize the total

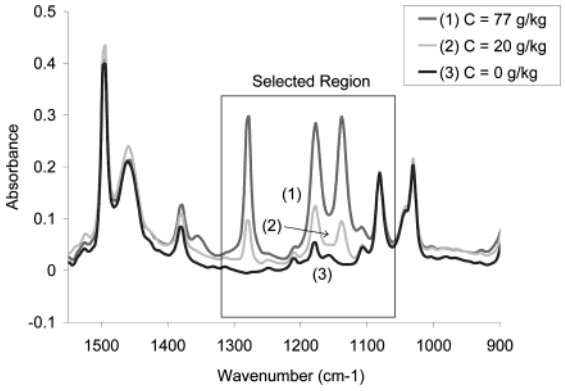

Figure 5. **Wavenumber region selected for calibration of absorbance spectra shown at three different concentrations.**

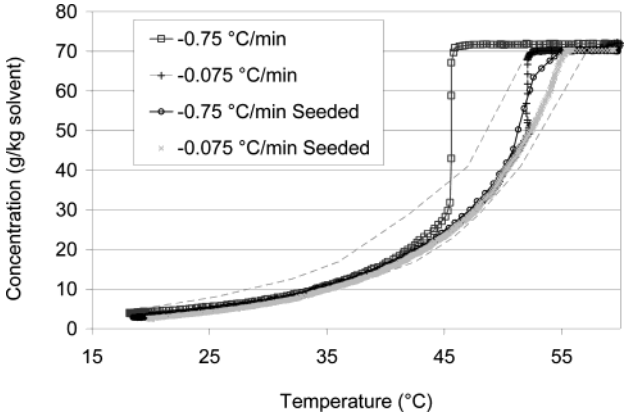

Figure 6. **Solution concentration profiles during the crystallization of pharmaceutical N at different cooling rates and seeding protocols. The dotted curves show the solubility and metastable limits at heating and cooling rates of 0.2 and −0.2 °C/min, respectively.**

prediction error in the model. For compound N, this corresponded to the region between wavenumbers 1060 and 1325 cm^{-1}, as shown in Figure 5. Finally, the calibration model was verified by using the "leave one out" and prediction of standards cross-validation procedures. The average prediction errors were 2.9 and 1.7%, respectively, for the two procedures, indicating an acceptable calibration.

4.1. Crystallization Monitoring. With the ATR-FTIR calibrated and linked to the AutoLab, several crystallizations with different cooling rates and seeding protocols were performed to study the impact of these process variables on crystal size. First, a solution of compound N in toluene was cooled from 70 to 20 °C at cooling rates of −0.75 and −0.075 °C/min. Then, these experiments were repeated with the introduction of 1% (w/w) seed material (median length approximately 75 μm) at 55 °C. The in situ solution concentration data (obtained from IR spectra) for the four experiments as a function of temperature are shown in Figure 6, with the solubility and metastable curves from Figure 3 shown as dotted curves for reference. Photomicrographs of the resulting crystals are shown in Figure 7.

The nonseeded experiments at the two cooling rates show a drop in solution concentration when their metastable limits are reached and primary nucleation occurs. The drop for the −0.075 °C/min cooling rate coincides with the metastable limit obtained during the AutoMeta experiment (−0.2 °C/

(7) Dunuwila, D. D.; Berglund, K. A. *J. Cryst. Growth* **1997**, *179*, 185.
(8) Lewiner, F.; Klein, J. P.; Puel, F.; Fevotte, G. *Chem. Eng. Sci*. **2001**, *56*, 2069.
(9) Tokalidou, T.; Fujiwara, M.; Patel, S.; Braatz, R. D. *J. Cryst. Growth* **2001**, *231*, 534.
(10) Nattkemper, A.; Schleiden, T.; Migliavacca, J. M.; Melin, T. *Chem. Eng. Technol*. **2003**, *26*, 881.
(11) Dunuwila, D. D.; Berglund, K. A. *Org. Process Res. Dev*. **1997**, *1*, 350.
(12) Togkalidou, T.; Tung, H.; Sun, Y.; Andrews, A.; Braatz, R. D. *Org. Process Res. Dev*. **2002**, *6*, 317.
(13) Inon, F. A.; Garrigues, J. M.; Garrigues, S.; Molina, A.; de la Guadia, M. *Anal. Chim. Acta* **2003**, *489*, 59.

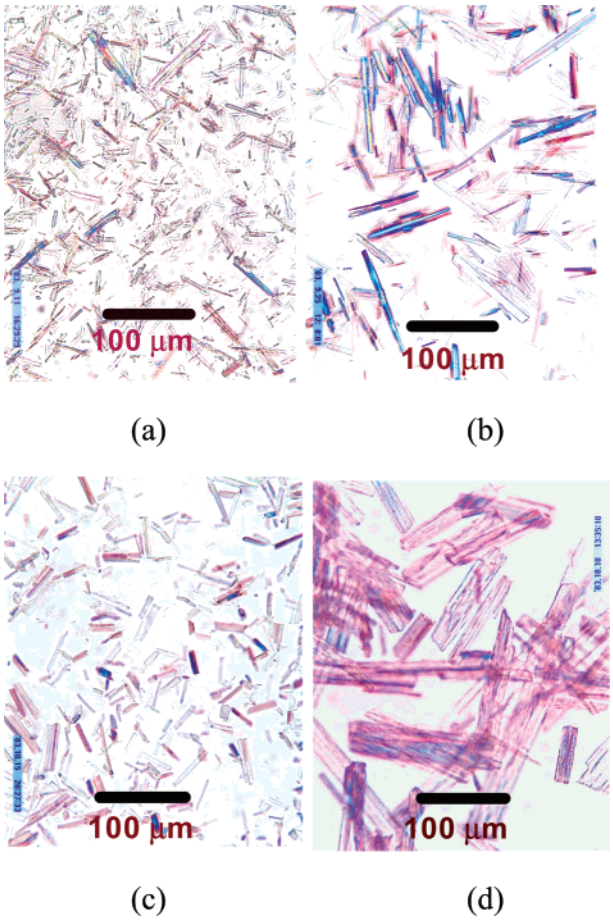

Figure 7. **Photomicrographs of crystals from crystallization experiments (a) Cooled at −0.75 °C/min, no seeding. (b) Cooled at −0.075 °C/min, no seeding. (c) Cooled at −0.75 °C/min, with 1% w/w seed. (d) Cooled at −0.075 °C/min, with 1% w/w seed.**

min cooling rate). However, at −0.75 °C/min, the metastable limit is observed at a lower temperature, resulting in a significantly larger drop in solution concentration. As expected, the product crystals with the faster cooling rate are considerably smaller (Figure 7a,b).

Alternatively, the seeded experiments run at the same cooling rates did not cross the metastable curve at any point during the crystallization. In comparison to Figure 7a and b, the seeded experiments at the same cooling rates are larger (Figure 7c,d), with the largest crystals resulting from the experiment that remained closest to the solubility curve (Figure 7d).

These results are consistent with the expectation of spontaneous crystal nucleation occurring at or beyond the metastable curve and provide a qualitative cause and effect relationship between process variables (such as cooling rate and seeding) and the crystal size. However, if a more quantitative understanding of these relationships is desired for optimal design of the crystallization process, supersaturation levels during the crystallization must be tracked.

5. Supersaturation Monitoring

Supersaturation is the primary driving force for crystallization processes. At high supersaturation levels, nucleation is the dominant mechanism, while growth is dominant at low supersaturation. As a result, product characteristics such as crystal size are a strong function of the supersaturation trajectory. Supersaturation (S) of a solute−solvent system is calculated by comparing the solution concentration at a given temperature (C) to the saturation concentration (C^*) at that temperature. Supersaturation has been represented either as a concentration ratio[3] ($S = C/C^*$) or as a concentration difference[14] ($S = C - C^*$), where the saturation concentration C^* is calculated on the basis of a curve fit of the solubility curve. For compound N, a fourth-order polynomial provides a suitable fit:

$$C^* = (5.242 \times 10^{-5})T^4 - (5.816 \times 10^{-3})T^3 + (0.258)T^2 - (4.949)T + 36.8$$

$$R^2 = 0.9999$$

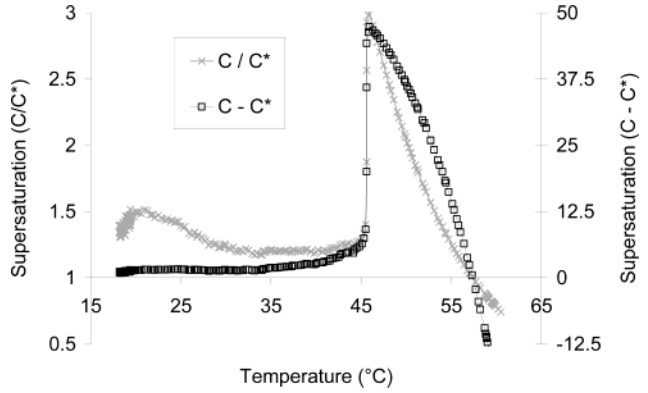

Figure 8. **Supersaturation calculated as a concentration ratio (left axis) and as a concentration difference (right axis).**

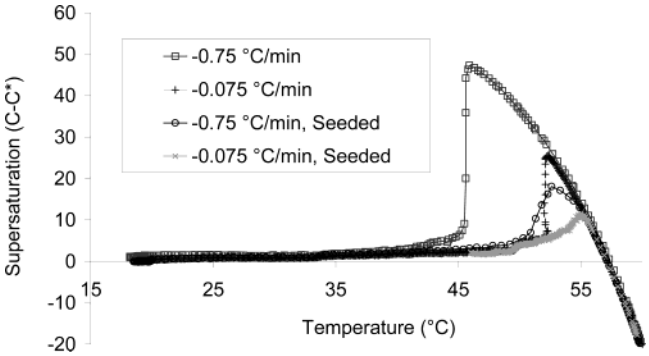

Figure 9. **In situ supersaturation levels during crystallization at different cooling rates and seeding protocols.**

The decision between using supersaturation as a ratio or difference in the current work was based on the relative error between the two calculations. Figure 8 shows supersaturation calculated in both ways for the nonseeded crystallization with the fast cooling rate of −0.75 °C/min. It is clear that any small inherent error in the concentration measurement is amplified with a ratio calculation at low temperatures (when C^* becomes small). The difference calculation is used in the remainder of this study.

The supersaturation profiles for the four experiments discussed in the previous section are shown in Figure 9. The first observation is that the resulting product crystal size

(14) Loffelmann, M.; Mersmann, A. *Chem. Eng. Sci.* **2002**, *57*, 4301.

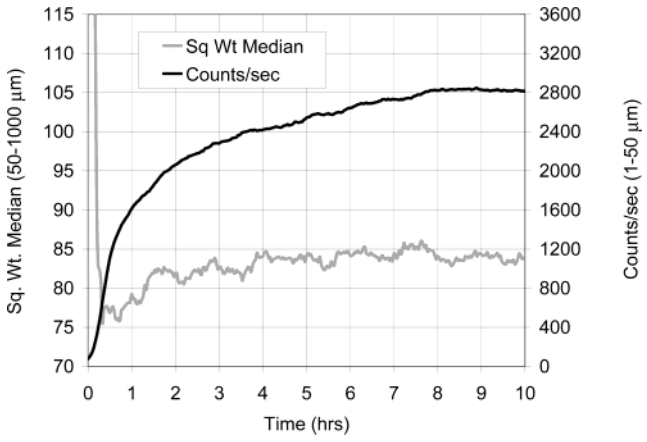

Figure 10. **Large-particle median and small-particle counts/s profile for the seeded crystallization at a cooling rate of −0.075 °C/min.**

(Figure 7a−d) correlates inversely with the maximum supersaturation level reached. A high level of supersaturation followed by rapid desupersaturation is characteristic of the nonseeded experiments and is indicative of a strong primary nucleation event. As a result, the product crystals are smaller than those produced in the corresponding seeded experiments.

The seeded experiment with the slow cooling rate (−0.075 °C/min) is the only case in which supersaturation gradually and continually drops from the seeding point (55 °C). However, a steady rise in the small particle counts/s, as measured by the FBRM (Figure 10), indicates that even with a constant slow cooling rate, secondary nucleation occurs throughout most of the cooling process. To minimize this mechanism and produce larger crystal sizes, it is apparent that a constant low level of supersaturation must be maintained throughout the crystallization. This is best achieved by implementation of a feedback supersaturation control strategy, as discussed in the next section.

6. Control of Supersaturation

In general terms, feedback control drives a process to operate in a manner that fulfills a predefined objective. The objective in this work was to maximize crystal growth by manipulating the reactor temperature to maintain supersaturation at a low value during the crystallization. The desired output from this strategy is a nonlinear temperature profile that maintains supersaturation at a chosen set point.

6.1. Cascaded Control Structure. The measurement-based scheme implemented to fulfill the control objective had a cascaded structure comprised of two proportional−integral control loops (Figure 11). At each time instant, the supersaturation measurement at the current system temperature was compared to the user-specified supersaturation set point. The primary loop minimized the error between the two by manipulating the cooling rate set point (constrained to between 0 and −1.0 °C/min). This new cooling rate was translated into a new reactor temperature set point by the AutoLab. The secondary loop ensured that the new temperature set point specified by the primary loop was achieved by manipulating the heater/chiller. In this way, the control system continually adjusted the reactor temperature to maintain supersaturation at the desired set point.

The advantage of a cascaded structure is a faster response compared to that with a single loop. However, this control scheme is only effective for processes with dynamics significantly slower than the dynamics of the entire control structure. This is due primarily to the time it takes for the heater/chiller temperature and reactor temperature to change in response to their new set points. For crystallizations, this limits the application of feedback control to growth-dominated processes as nucleation events usually occur faster than the control scheme can respond.

As with any cascaded control tuning strategy, the primary loop was tuned once acceptable performance was achieved with the secondary loop. Initial estimates for the primary loop control parameters were obtained by monitoring the response of supersaturation to a step change in cooling rate and applying the process reaction curve method.[15]

Once the control structure was tuned, the following procedure was implemented. The initially undersaturated solution was cooled to within the metastable zone (55 °C) and seeded with 1% (w/w) seed, as in the monitoring experiments discussed previously. Supersaturation control was activated by initiating a new step in the AutoLab that engaged the primary controller.

6.2. Control Results and Discussion. As the control objective was to maximize growth, low set-point values for supersaturation were specified. Results for supersaturation set points of $S = C - C^* = 2.0$ and 1.5 are shown in Figure 12a and b, respectively. In both cases, the controller was constrained to a 0 °C/min cooling rate at the beginning of the control experiment to allow the system to desupersaturate to the set-point value. The control structure did well to maintain the supersaturation at the desired level throughout most of the control experiment by continually adjusting the reactor temperature. Consistent with optimal temperature trajectories,[16] the reactor temperature followed a convex profile in both cases.

Towards the end of both control experiments, the control structure had difficulty maintaining the supersaturation at the set-point value. The departure from set point coincided with the onset of secondary nucleation, which was detected by a rise in the FBRM small particle counts/s, as shown in Figure 13a and b. As mentioned earlier, the speed of the controller response is not sufficient to keep up with the dynamics of this mechanism. In both cases, secondary nucleation became more probable as the crystallization progressed because the slurry density increased and the metastable zone narrowed. The extent of secondary nucleation was reduced for the $S = 1.5$ case because its concentration profile is close to the solubility curve. Nonetheless, in comparison to the small counts profile in Figure 10 (seeded and cooled at −0.075 °C/min without control), the controlled experiments resulted in a marked reduction in the measured particle counts/s. Further evidence that nucleation was suppressed in the

(15) Stephanopoulos, G. *Chemical Process Control*; Prentice Hall: New Jersey, 1984.
(16) Mullin, J. W. In *Crystal Growth*; Pamplin, B. R., Ed.; Pergamon Press: New York, 1980.

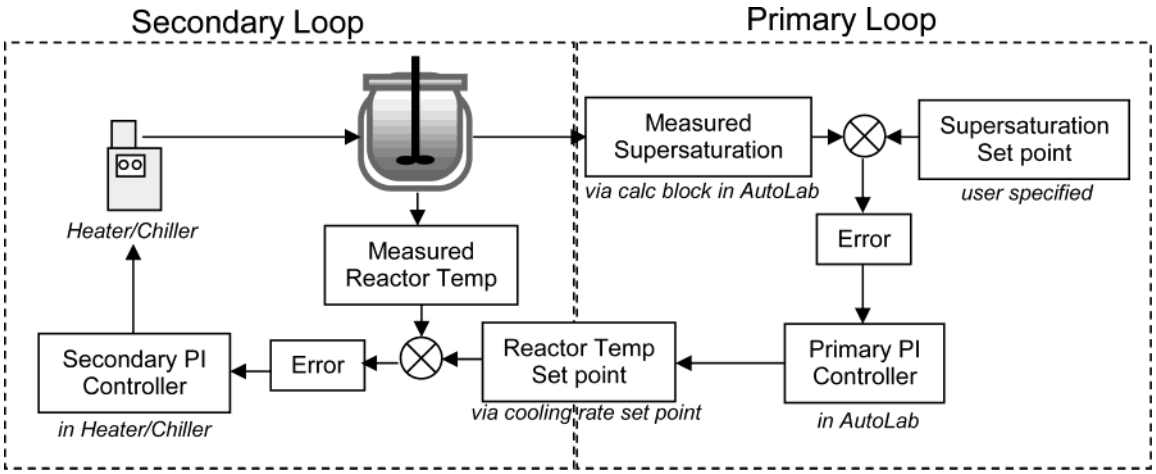

Figure 11. **Cascaded feedback control scheme for supersaturation control.**

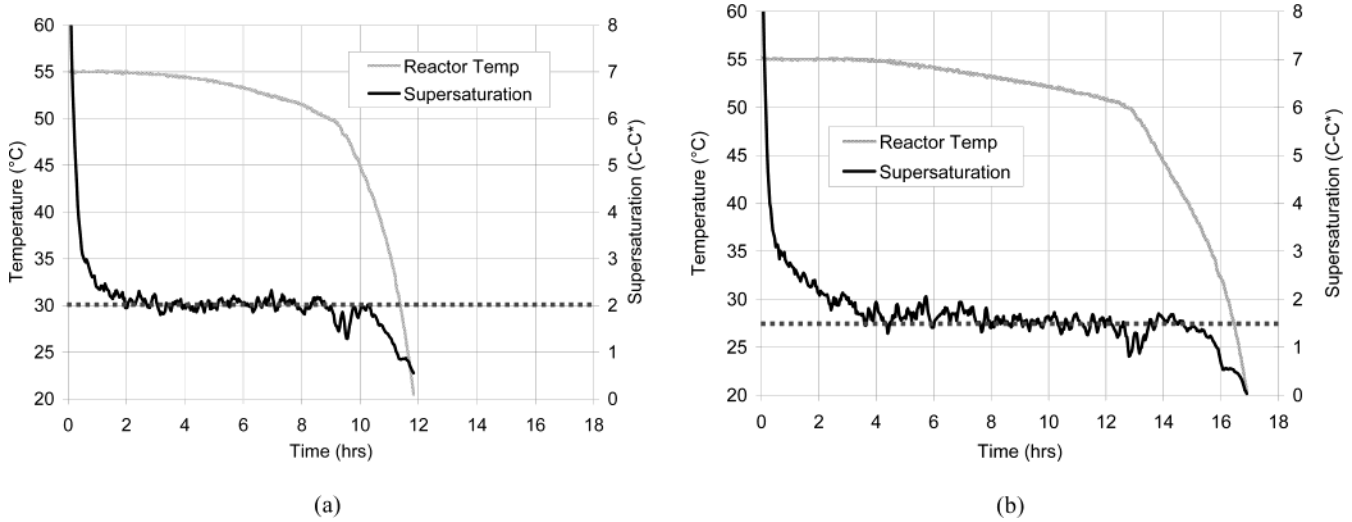

Figure 12. **Supersaturation and temperature profiles for control experiments with supersaturation set-point values of (a) 2.0 and (b) 1.5.**

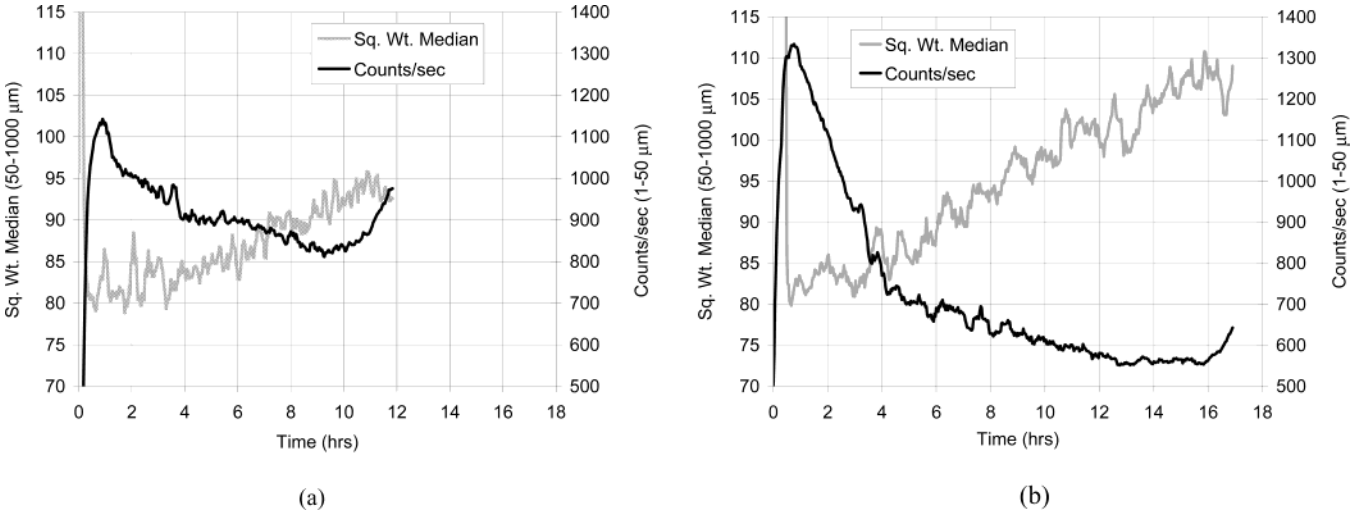

Figure 13. **Large-particle median and small-particle count profiles for control experiments with a supersaturation set-point value of (a) 2.0 and (b) 1.5.**

controlled experiments is obtained by considering the FBRM square weighted median of particles between 50 and 1000 μm, a statistic sensitive to crystal length. These trajectories in Figure 13a and b for the controlled experiments demonstrate that the crystals grew steadily throughout the experiment. The same FBRM statistic shows that this did not occur in the experiment without feedback control (Figure 10).

Finally, the photos of the crystals grown in the two controlled experiments are shown in Figure 14a and b. In comparison to the particles in experiments without control (Figure

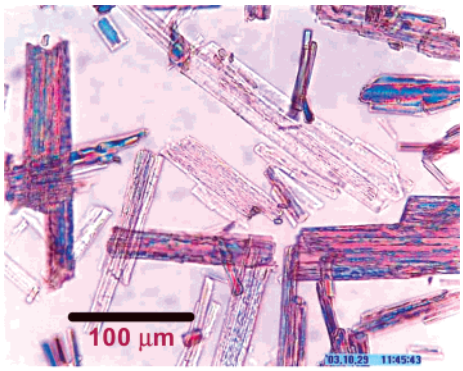

(a)

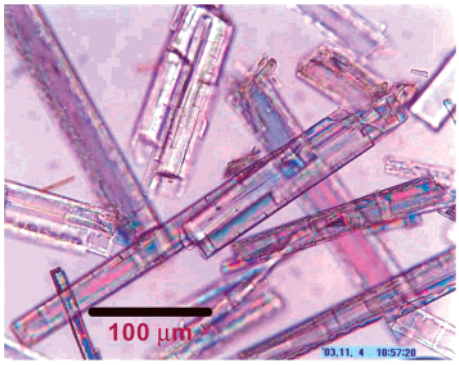

(b)

Figure 14. **Photos of crystals for control experiments with a supersaturation set-point value of (a) 2.0 and (b) 1.5.**

7a−d), the particles obtained are significantly larger. As expected, the growth is more pronounced in the $S = 1.5$ case, leading to a larger and more uniform crystal size population.

7. Conclusions

The experimental work described in this report demonstrates the use of automation, in situ laser backscattering technology, and ATR-FTIR spectroscopy in the real-time monitoring and control of a pharmaceutical crystallization process. First, solubility and metastable curves were determined in automated fashion using a laser backscattering probe coupled with an automated reactor system. The resulting metastable zone defined the operating window for promoting crystal growth during crystallization. Second, real-time concentration data from several cooling crystallizations were obtained via a PLS calibration technique applied to FTIR spectra. Experimental data for several crystallizations demonstrated a connection between small crystals in the product and a nucleation event early in the process. This relationship was corroborated by in situ supersaturation measurements, calculated as the difference between solution concentration and saturation concentration at the system temperature. Finally, real-time supersaturation control was implemented to favor crystal growth over nucleation throughout the experiment. This was realized via a feedback control scheme involving a primary loop to determine a set point for cooling rate and a secondary loop to manipulate the heater/chiller to maintain the specified cooling rate. Control experiments worked well to maintain the system at a desired low supersaturation level, producing significantly larger crystals. This is a marked improvement over the wide crystal size range obtained during early development. Although the focus of this work was to target large crystal sizes, cases do arise where an intermediate crystal size range is desired to improve drug substance dissolution or drug product processing. Such objectives can be realized with the current methodology by specifying higher supersaturation set points than those used in this study.

The outcome of the laboratory work presented here can be of benefit to manufacturing plants even if they are not configured for supersaturation control. For instance, the large-scale crystallizer can be programmed to follow the nonlinear temperature trajectory obtained from the laboratory control experiment. For plants without nonlinear temperature profiling capabilities, this can be approximated by using a series of linear ramps. Finally, the application of this work is not limited to cool-down crystallizations, as the same techniques can be modified and applied to antisolvent and evaporation crystallizations as well.

Acknowledgment

We thank Robert Brush of Mettler-Toledo for assistance with the ATR-FTIR instrumentation and Jeremy Eberhardt for his contribution to the experimental work.

Received for review February 20, 2004.

OP049959N